MM Science Journal | www.mmscience.eu
ISSN 1803-1269 (Print) | ISSN 1805-0476 (On-line)
Special Issue | TEAM 2024
Transdisciplinary and Emerging Approaches to Multidisciplinary Science
11.9.2024 – 13.9.2024, Ostrava, Czech Republic
DOI: 10.17973/MMSJ.2024_10_2024064

TEAM2024-00004

EFFECT OF BUILD POSITION ON SURFACE ROUGHNESS OF SLM PRINTED INCONEL 718

PREETI GAUTAM[1*], JIRI HAJNYS[1], JAKUB MESICEK[1], AKASH NAG[1], QUOC-PHU MA[1], JANA PETRU[1]

[1]Faculty of Mechanical Engineering, VSB - Technical University of Ostrava, Ostrava, Czech Republic
*Corresponding author; e-mail: preeti.gautam.st@vsb.cz

Abstract
The present work investigates the variation of the surface roughness due to the build position of specimens with respect to the inert gas flow direction and re-coater movement direction. Selective laser melting (SLM) method was used to study this effect using Inconel 718 as workpiece material. A total of 21 samples were placed equidistant from each other on the built plate to observe the effect of gas flow and re-coater movement. The effect of these parameters on the printed samples was analyzed in terms of the profile surface roughness parameter such as Ra and Rz in the build direction. The result showed that samples placed near the gas inlet and the re-coater starting position had larger roughness as compared to the samples placed further from the gas inlet and re-coater end position. The result showed that the profile average roughness parameter values varied from Ra = 5.02 µm to 14.7 µm and profile maximum height surface parameter varied from Rz = 47.61 µm to 118.3 µm for all the printed samples. Surface topography of the samples was also studied which showed common printing defects such as cracks, micropores, local solidified melt pools, and dimples. The study opens an avenue to explore and optimize the placement of the printing sample on the build plate with respect to the inlet gas flow and re-coater movement directions for better surface roughness.

Keywords:
Additive manufacturing; Inconel 718; SLM; Surface roughness.

1 INTRODUCTION

Additive manufacturing is a method where 3D parts are created by adding layers of material based on digital 3D design data [Kolomy et al. 2023]. This process employs either fine powder or filament raw material [Kozior et al. 2023, Opěla et al. 2023]. This innovative manufacturing process enables experts to design intricate components that would be challenging to produce using conventional methods [Srivastava et al. 2023]. The novel manufacturing approach faces several challenges such as achieving precise dimensions, addressing issues related to poor ductility, managing high surface roughness, and mitigating the formation of residual stress within the parts [Marsalek et al. 2019, Tolochko et al. 2003]. Selective laser melting (SLM) [Gupta et al. 2023] is a widely used manufacturing technology to create metallic components that allow greater design freedom to create components with complex shapes that are difficult or expensive to achieve by traditional methods [Jia et al. 2014]. Considering the advanced manufacturing capabilities of the SLM process, it can be regarded as a highly promising method for producing nickel-based superalloy components such as Inconel 718 alloy due to its advantages over traditional subtractive methods, including superior design flexibility and reduced material waste [Baicheng et al. 2017]. The literature review reports that the fabrication of Inconel 718 components through the SLM process produced better mechanical properties such as creep resistance and fatigue strength compared to that produced using traditional manufacturing methods [Brown et al. 2018, Dadbakhsh et al. 2010, Mesicek et al. 2021]. The Inconel 718, Ni superalloy can be used in various applications that require the fabrication of working parts that require high corrosion and high strength resistance at higher temperatures such as aeronautics, jet engine components, chemical and energy industries for safety valves, packers, and flow control devices due to excellent mechanical properties [Bhavsar et al. 2001, Donachie et al. 2002, Majerik et al. 2023, Qi et al. 2009]. The mechanical characteristics of the structural bearing have varied because of anisotropy in the material. Although having superior mechanical properties, the samples printed through SLM face bottlenecks in their acceptance in industries due to the inadequate surface condition of the printed parts. Therefore, in the last few years, many authors tried to investigate the main reasons and methods to overcome this issue [Barenyi et al. 2023]. [Kaynaka, Tascioglu et al. 2018] investigated the effect of surface roughness, microhardness, and residual stresses on an as-built sample of Inconel 718 by the SLM method. All printing parameters were kept the same except feed rate which had three different values. It was observed that an increase in

feed rate led to an increase in surface roughness. The lower feed rate generating, and lesser surface roughness value ranged from 19 to 24 µm for as-built samples. [Lesyk et al. 2020] studied the effects of mechanical surface roughness, hardness, porosity, and residual stress on an as-built sample of Inconel 718 by the SLM method and compared the results with the different post-processing methods. It was observed that as an in-built condition surface roughness, the Ra value was 5.27 µm and after the post-processing, values for roughness parameters Ra and Rz were decreased. Ramanathan et al. [Balachandramurthi et al. 2018] manufactured samples from Inconel 718 powder using electron beam melting and SLM methods. The samples produced through these methods underwent machining followed by heat treatment (HT) and Hot Isostatic Pressing (HIP). Some samples underwent the combined HIP and HT process, both in the as-built condition and on the machined surfaces and some only underwent either HIP or HT for both fabrication methods. It was observed that samples manufactured through the EBM method exhibited a surface roughness approximately three times higher in comparison to those produced through the SLM method and the machined surfaces exhibited the lowest roughness among all conditions. Bean et al. used SLM for manufacturing Inconel 718 of 370 W. Throughout the experiment, the impact of shifting the laser focus and built position of samples on surface roughness, density, and porosity was observed. The samples further underwent a two-step heat treatment process. The results indicated that, after these heat treatment processes, the surface roughness was reduced to as low as 28 %. This outcome suggests that the adjustment of laser focus and built sample position, along with the specified heat treatment steps, significantly influenced the surface characteristics of the Inconel 718 samples.

Although several studies related to understanding the effect of various technological parameters on the surface roughness of the printed parts have been carried out. However, studies related to the effect of sample positioning on the built plate with respect to the inert gas flow direction and re-coater movement direction on the printed sample surface roughness are sparsely available in the open literature. Therefore, in this study, Inconel 718 samples distributed evenly across the built plate were printed by the SLM method, and the resultant surface roughness of the samples was examined in as built condition. The profile average surface roughness parameter (Ra) and maximum surface roughness parameter (Rz) were used to examine the surface quality.

2 MATERIALS AND METHOD

In this study, Inconel 718 powder was used, having an average powder particle size of approximately 15-40 µm. Most of the powder particles had spherical shapes. The chemical composition of Inconel 718 powder is given in Table 1.

Tab. 1: Elemental composition of Inconel 718 powder [17].

Element	Ni	Mo	Nb	Cr	Ti	Al	Co	C
Mass (%)	53.5	3.05	5	20	0.98	0.58	0.98	0.046
Element	Mg	Si	P	Su	B	Cu	Fe	
Mass (%)	0.33	0.32	0.013	0.012	0.005	0.29	Balance	

The specimens in the form of stripes were designed in Inventor Professional, having dimensions of 40 mm x 10 mm x 3 mm. In total 21 specimens of the same dimension were designed. Renishaw 500 Flex, an SLM-based printer was used in the present study. Specimen geometry, gas flow direction, build direction, and re-coater direction are shown in Fig 1. Specimens were printed using the optimal technological parameters suggested by the OEM to investigate the surface roughness of the samples under an argon atmosphere. The technological parameters used during printing are shown in Table 2. All 21 specimens were placed equidistance from each other on the built plate to observe the effect of sample positioning on surface finish. The build chamber consists of a material delivery platform, a building platform, and a coater blade that is used to force the new powder across the build platform. Before starting the printing process, the building substrate was pre-heated to 170 °C to minimize distortion in the sample. After spreading the uniform layer of the powder, a focused laser beam locally melts the metal powder and carves the layers of the material. After each new powder layer spread, the high-power laser beam melts the new powder layer and partially melts the pre-solidified layers. This allows us to fuse the previous layers with the new layer. This process repeats and allows the development of complex shapes easily [Mechali et al. 2024].

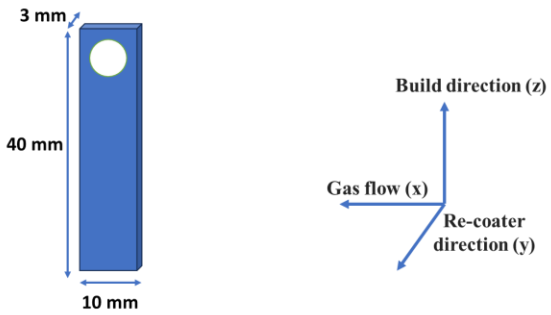

Fig. 1. Specimen geometry of Inconel 718 material.

Tab. 2. Printing parameters for Selective laser melting (SLM) process.

Power	Scanning speed	Hatch distance	Layer thickness
200 W	650 mm/s	0.09 mm	0.06 mm

Fig. 2 shows the distribution of the samples on the build plate during the printing process. The assisted gas flow direction and the re-coater movement direction with reference to the build plate are also shown in Fig. 2b. Samples are placed in equidistant rows with 4 and 5 samples in each alternative row and the last row having 3 samples from the re-coater direction. The samples were also placed in alternative columns to optimize print conditions and to have equal distances within each sample. Fig. 2b also shows the sample number arranged in rows for easy identification and post-printing evaluations.

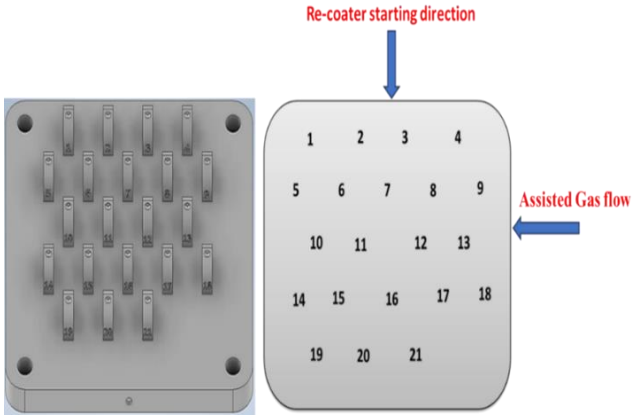

(a) **(b)**

Fig. 2: (a) The build position of specimens on the build plate and figure, (b) The gas flow direction and re-coater direction on the distribution of specimens.

After completion of the printing process, all the samples were cut from the build plate with a wire electro-discharge machine [Srivastava et al. 2019] for precise cutting.

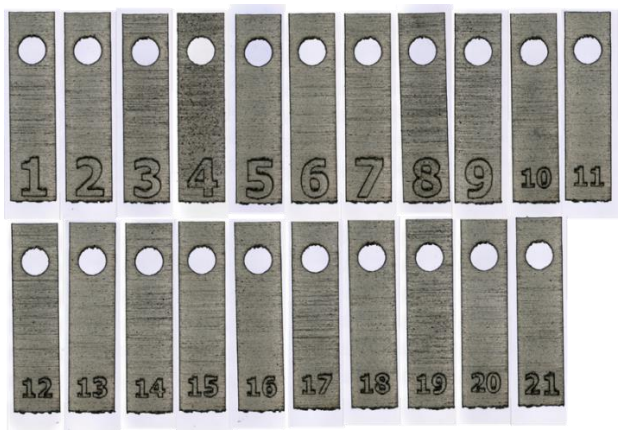

Fig. 3: SLM printed sample shown after cutting by WEDM.

Investigation of the surface topography and surface roughness of the printed specimens was carried out using an optical microscope (OM) and non–contact profilometer. The sample surfaces were first captured using a Keyence VHX-6000 digital optical microscope to observe the surface topography of the as-built surfaces of the specimens. 50X optical zoom objective having 0.006 µm vertical resolution and 0.625 µm lateral resolution was used to capture the surface details An area of 7 mm x 5 mm was captured. Further, a MircroProf FRT profilometer was used to measure the profile roughness parameters. A total area of 16 mm x 4 mm was scanned for each printed specimen. The scanned data was imported to MountainsMap surface analysis software, where surface roughness values were measured. In the present study, profile surface roughness parameters such as arithmetic mean height (Ra) and maximum height (Rz) were evaluated to understand the surface finish of the printed specimens. The roughness measurements were carried out according to ISO 21920 using an S-filter of 2.5 µm, an L-filter of 2.5 mm, and a total evaluation length of 12.5 mm.

3 RESULT AND DISCUSSIONS

3.1 Profile Surface roughness measurement

The profile roughness parameters Ra and Rz for all printed specimens are shown in Fig. 4a and 4b, respectively. The vertical bars show the magnitude of the roughness for each specimen in the same position as printed on the built plate, as shown in Fig. 2. The variation of the surface roughness not only affects the part appearance but also affects the mechanical property of the printed part such as fatigue strength and high-cycle fatigue life.

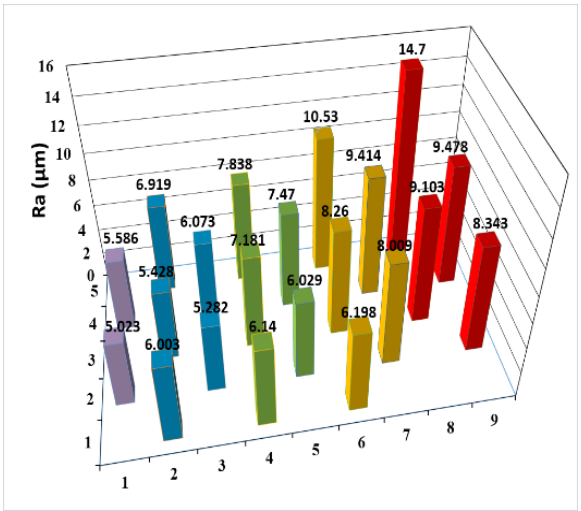

(a)

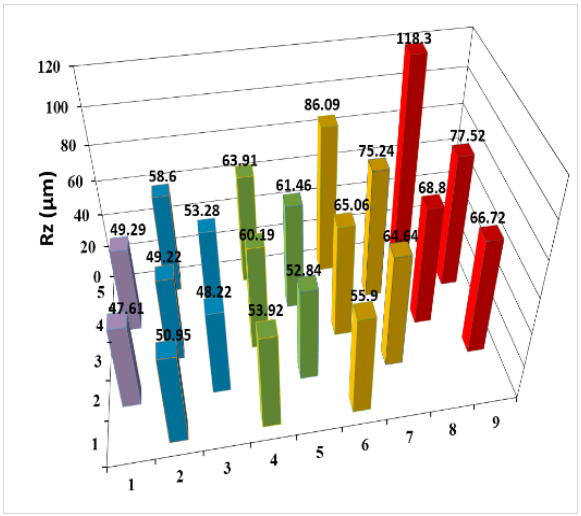

(b)

Fig. 4: (a) The measured roughness Ra values are the build position of Inconel 718 specimens, and (b) the Rz value is the build position of Inconel 718 specimens.

The paper size is the A4 (210mm x 297mm). Set the page margins to 20 mm for the top margin and 18 mm for bottom, 20 mm for left, and 20 mm for right. For the present study, both Ra and Rz roughness parameters show a decreasing trend with a larger distance from the inert gas flow inlet and re-coater starting positions. The highest profile roughness parameter values (Ra = 14.7 µm and Rz = 118.3 µm) were obtained for specimen number 4, which was located at the right upper corner of the built plate nearest to the gas inlet and re-coater starting position.

The lowest roughness magnitude was measured for sample 14, having Ra = 5.02 µm and Rz = 47.61 µm. It was also observed that the roughness values decrease within the same row as the sample position distance increases from the gas inlet. This phenomenon can be attributed to the quick solidification of the melted powder due to the proximity of the sample to the gas inlet. The variation in the solidification times between the layers, depending on the region of heat flow, causes different thermal gradients to exist in between the layers in SLM. This difference in heterogenous solidification during the printing process causes variation in the surface roughness of the parts [Ross et al. 2024]. Moreover, the quick solidification of the layers also results in poor adhesion between powder layers, affecting porosity, microstructure, and mechanical properties. Therefore, the samples near the inlet gas flow (Sample 2, 3, 4, 7, 8, 9, 11, 12, 13, 16, 17, 18, 20 and 21) due to quicker solidification rate showed a higher magnitude of surface roughness as compared to the samples farther from the inlet (Sample 1, 5, 6, 10, 14, 15 and 19) due to the diminished gas flow effect. Another phenomenon affecting the surface roughness was also observed when comparing the surface roughness of the samples at the same distance from the gas inlet position. It was observed that the samples closer to the powder re-coater starting position showed higher surface roughness than those farther from the re-coater. This can be attributed to the spreading of the powder from the top to the bottom part of the built plate. Initially, the amount of powder in the re-coater blade is larger at the top, and due to the gas flow from the right side, some powder particles may flutter and adhere to the samples nearby. Therefore, the uneven spreading of the powder on the built plate and directional melting of the powder from one direction causes non-uniform solidification and adhesion of the layers, increasing the surface roughness of the samples positioned on the top side or nearer to the re-coater starting position. Finally, the combined effect of the inlet gas flow and the powder spreading direction leads to the variation of the roughness from the top right-side samples showing the highest roughness and the bottom left samples showing the least roughness. However, one exception to this trend was seen for samples 19, 20, and 21. These samples showed a higher roughness magnitude compared to the samples printed in the row above it (Sample 14, 15, and 16). This variation in the trend can be due to the missing sample near the inlet flow chamber, which failed to resist the flow interacting with samples 19, 20, and 22. Therefore, an increased surface roughness was observed in the last row. However, the roughness trend decreased from right to left with the same row due to the same reason mentioned earlier. The results showed that controlling and optimizing gas flow parameters and positioning of the samples on the build plate is essential for achieving the desired quality and performance of the printed samples.

3.2 Surface Topography

Fig. 5 shows the surface topography (top view), 3D views, and profile roughness curve for as-built SLM manufactured samples 4 (a, b, c) and 14 (d, e, f). Samples 4 and 14 were selected for detailed study as they showed the highest and lowest surface roughness values, respectively. The top view of the samples showed specific surface features generated by using the SLM methods, such as burnt area, micropores, cracks, and melted zones [Korkmaz et al. 2022]. The surface generated in sample 4 shows partially melted powder and spatters sticking to the sample surface due to the existence of the heat-affected zone. The figure also shows a region of the elongated melt pool, which can be the result of non-uniform solidification and non-adhering between two melted layers. Also, a surface spatter is observed in which small droplets of molten metals are expelled and formed during the melting of the powder, which then sticks to the sample surface in the form of a spatter and deteriorates the sample surface. Due to the close proximity of the sample to the inlet gas chamber, a higher temperature gradient occurs in the sample, inducing thermal stresses leading to the generation of surface cracks, which can be observed in the surface. Also, the surface topography shows signs of localized burnt area, which can be attributed to the excessive laser power or prolonged exposure leading to local excessive melting and burn-through, leading to higher surface roughness. In some parts, balling defects can also be observed, which are due to the accumulation of the un-melted powder and the formation of a spherical mass on the surface of the printed part. Surface porosities are also observed in the sample surface, which is formed due to non-proper melting or gas entrapment during the printing process, leading to poor surface finish and weakened mechanical properties. The 3D view shown in Fig. 5b shows the presence of regions with high peaks and deep valleys throughout the investigated area. The presence of these regions is due to several reasons explained above, which increase the overall surface roughness of the printed parts. The presence of a higher magnitude of surface roughness limits the wide acceptability of the printed parts in practical applications. The higher variation in the surface profile throughout the sample can be more easily identified by the roughness profile shown in Fig. 5c. The overall surface profile varies from 150 µm above the reference plane and -100 µm below the reference plane. This observation of the roughness profile corresponds to the higher surface roughness values measured for sample 4. Sample 14 shows a uniform surface without many defects, resulting in lower surface roughness. Some defects, such as localized surface cracks, burnt areas, and micro holes, are observed in the printed sample surface. The uniformity in the surface is mainly due to the distance of the sample from the gas inlet chamber and the re-coater starting position. This increased distance lowers the gas flow interacting with the sample, lowering the solidification rate and thermal gradient between the layers. Also, the 3D view of the sample shows a uniform surface throughout the scanned area. The absence of high peaks and deep valleys is observed in the figure. Also, the roughness profile shows the variation of the surface throughout the printed sample ranges within 50 µm above and below the reference plane in contrast to sample 4, having a range of 250 µm from the deepest valley to the highest peak. These differences in the measured surface finish between the samples are mainly due to the sample position on the build plate during printing relative to the inlet gas flow and re-coater movement direction.

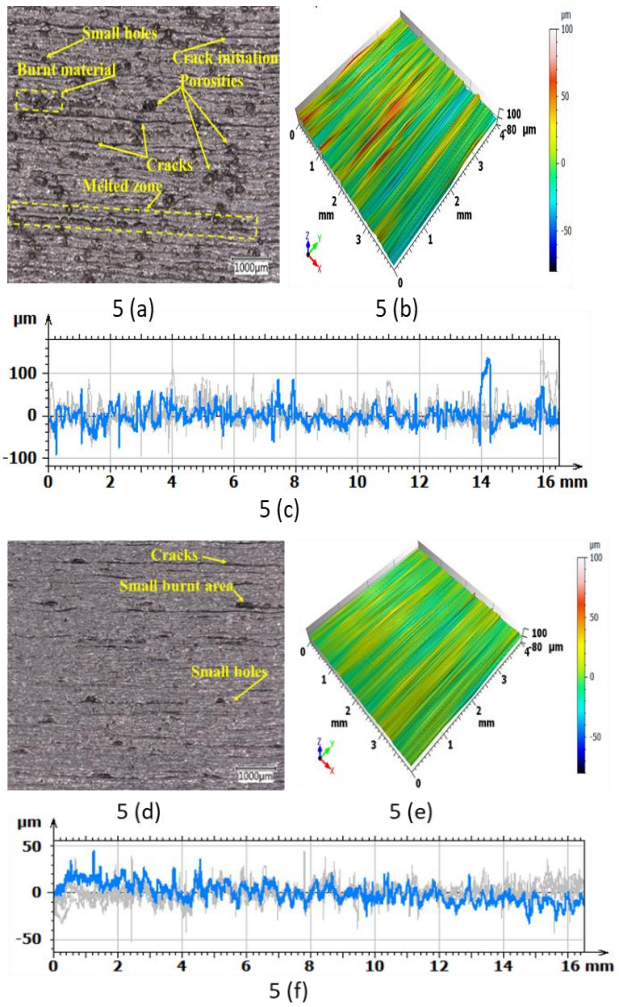

Fig. 5: (a) Sample 4: Surface topography, (b) Sample 4: 3D view, (c) Sample 4: profile roughness, (d) Sample 14: Surface topography, (e) Sample 14: 3D view, (f) Sample 14: profile roughness.

4. CONCLUSION

In this study, the SLM method was utilized to additively fabricate specimens using Inconel 718 material. A total of 21 samples were fabricated, with a specific arrangement strategy on the build plate. The effect of the inlet gas flow direction and re-coater direction was studied in terms of generated surface roughness on their as-built condition. The main findings of the study are summarized as follows:

The results showed that the profile surface roughness parameters Ra and Rz values decrease with an increase in the distance of the sample position from the inlet gas flow direction. This is attributed to the faster rate of solidification of the layer, limiting uniform fusing of the layers.

The surface finish of the samples is also affected by the distance of the sample position from the re-coater starting position due to unevenness in the spreading of the powder over the built plate.

The highest value of Ra and Rz was measured as 14.4 µm and 118.6 µm, respectively, for sample 4, which was closest to the inlet gas flow direction and re-coater starting position.

The lowest value of Ra and Rz was measured as 5.02 µm and 47.6 µm, respectively for sample 14 which is farther from the inlet gas flow direction and re-coater starting position.

The surface topography images showed typical printing defects on the surface of the printed samples, such as cracks, micropores, local burnt area, and melted zone, attributing to non-uniform adhesion and the formation of thermal gradient between the consecutive layers.

In future studies, effect of build orientation along with sample positioning can be carried out due to its effect on surface roughness. In the current study, the samples were printed vertically which showed a wider range of surface roughness which may be lowered for samples printed in horizontal orientation due to stacking horizontally, facilitating better fusion between layers and a smoother surface finish.

5. FUNDING

This study was conducted in association with the project Innovative and Additive Manufacturing Technology—New Technological Solutions for 3D Printing of Metals and Composite Materials (reg. no. CZ.02.1.01/0.0/0.0/17_049/0008407) financed by Structural Funds of the European Union. Article has been done in connection with project Students Grant Competition SP2024/087 „Specific Research of Sustainable Manufacturing Technologies “financed by the Ministry of Education, Youth and Sports and Faculty of Mechanical Engineering VŠB-TUO.

REFERENCES

[Baicheng 2017] Baicheng, Z., et al. Study of selective laser melting (SLM) Inconel 718-part surface improvement by electrochemical polishing. Materials & Design, February 2017, Vol. 116, pp 531–537. ISSN 0264-1275

[Balachandramurthi 2018] Balachandramurthi, A. R., et al. Influence of defects and as-built surface roughness on fatigue properties of additively manufactured Alloy 718. Materials Science and Engineering: A, September 2018, Vol. 735, pp 463–474. ISSN 0921-5093

[Barenyi 2023] Barenyi, I., et al. Processing of Bimetallic Inconel 625-16Mo3 Steel Tube via Supercritical Bend: Study of the Mechanical Properties and Structure. Materials, October 2023, Vol. 16, No. 20, pp 6796. ISSN 1996-1944

[Bhavsar 2001] Bhavsar, R. B., et al. Use of alloy 718 and 725 in oil and gas industry. Minerals, Metals and Materials Society/AIME, Superalloys 718, 625, 706 and Various Derivatives(USA), pp 47–55.

[Brown 2018] Brown, D., et al. Surface integrity of Inconel 718 by hybrid selective laser melting and milling. Virtual and Physical Prototyping, October 2017, Vol. 13, No. 1, pp 26–31. ISSN 1745-2759

[Dadbakhsh 2010] Dadbakhsh, S., et al. Surface finish improvement of LMD samples using laser polishing. Virtual and Physical Prototyping, November 2010, Vol. 5, No. 4, pp 215–221. ISSN 1745-2759

[Donachie 2002] Donachie, M. J. and Donachie, S. J. Superalloys: a technical guide. ASM international. 2002

[Gupta 2023] Gupta, M. K., et al. Tribological characteristics of additively manufactured 316 stainless steel against 100 cr6 alloy using deep learning. Tribology International, October 2023, Vol. 188, pp 108893. ISSN 1879-2464

[Jia 2014] Jia, Q. et al. Selective laser melting additive manufacturing of TiC/Inconel 718 bulk-form nanocomposites: Densification, microstructure, and performance. Journal of Materials Research, July 2014, Vol 29, pp 1960–1969.

[Kaynak 2018] Kaynak, Y. et al. Finish machining-induced surface roughness, microhardness and XRD analysis of selective laser melted Inconel 718 alloy. Procedia Cirp, Vol. 71, pp 500–504.

[Kolomy 2023] Kolomy, S. et al. Influence of Aging Temperature on Mechanical Properties and Structure of M300 Maraging Steel Produced by Selective Laser Melting. Materials, Vol. 16, pp 977.

[Korkmaz 2022] Korkmaz, M. E. et al. Development of lattice structure with selective laser melting process : A state of the art on properties, futurs trends and challenges. Journal of Manufacturing Processes, Vol 81, p. 1040–1063.

[Kozior 2023] Hanon, M. M. et al. Evaluation of the Influence of Technological Parameters of Selected 3D Printing Technologies on Tribological Properties. 3D Printing and Additive Manufacturing, Vol 11, pp 2329-7670 ISSN 2329-7662

[Lesyk 2020] Lesyk, D. A. et al. Post-processing of the Inconel 718 alloy parts fabricated by selective laser melting: Effects of mechanical surface treatments on surface topography, porosity, hardness and residual stress. Surface and Coatings Technology, July 2020, Vol. 381, pp 125136, ISSN 0257-8972

[Maierik 2023] Majerik, J. et al. Analysis of the technological process of welding a membrane wall with Inconel 625 nickel alloy. The International Journal of Advanced Manufacturing Technology, June 2023, Vol. 127, pp 30313048

[Marsalek 2019] Marsalek, P. et al. Virtual prototyping of 3D printed cranial orthoses by finite element analysis. In AIP Conference Proceedings. Aip Publishing 2116, 320010

[Mechali 2024] Mechali, A. et al. ABRASIVE SURFACE TREATMENT OF ALSI10MG PARTS MADE BY L-PBF.

February 2024, pp 7165-7172, MM Science Journal

[Mesicek 2021] Mesicek, J. et al. Abrasive surface finishing on SLM 316L parts fabricated with recycled powder. Applied Sciences, Vol 11, pp 2869.

[Opela 2023] Opěla, P. et al. High Cycle Fatigue Behaviour of 316L Stainless Steel Produced via Selective Laser Melting Method and Post Processed by Hot Rotary Swaging. Materials, 2023, Vol 16, pp 3400.

[Qi 2009] Qi, H. et al. Studies of standard heat treatment effects on microstructure and mechanical properties of laser net shape manufactured Inconel 718. Metallurgical and Materials Transactions A, 2009, Vol 40, pp 2410–2422.

[Ross 2024] Ross, N. S., et al. A new intelligent approach of surface roughness measurement in sustainable machining of AM-316L stainless steel with deep learning models. Measurement, 2024, Vol, pp 114515.

[Srivastava 2023] Srivastava, A. K., et al. Research Progress in metal additive manufacturing: Challenges and Opportunities. International Journal on Interactive Design and Manufacturing (IJIDeM), 2023, Vol, pp 1–17.

[Srivastava 2019] Srivastava, A. K., et al. Surface integrity in wire-EDM tangential turning of in situ hybrid metal matrix composite A359/B4C/Al2O3. Science and Engineering of Composite Materials, Aug 2019, Vol 26, pp. 122–133.

[Tolochko 2003] Tolochko, N. K., et al. Mechanisms of selective laser sintering and heat transfer in Ti powder. Rapid prototyping journal, December 2003, Vol 9, pp 314–326, ISSN 1355 2546.